



Analysis of Surface Alignment of SWCNTs–DNA based Nanobiosensors



Sergi Civit¹ and Sonia Trigueros^{2*}

¹Department of Genetics, Microbiology and Statistics (UB), University of Barcelona, Spain

²Department of Zoology, University of Oxford, UK

*Corresponding author: Sonia Trigueros, Department of Zoology, Oxford University, OX13PS Oxford, UK, Email: sonia.trigueros@zoo.ox.ac.uk

Submission: 📅 November 02, 2018; Published: 📅 November 13, 2018

Abstract

Nanomaterials offer several significant advantages owing to their small size. High surface area/volume ratios allow for stronger signals, better catalysis and more rapid diagnostic of analytes, as well as enhanced optical properties. These nanoscale properties represent considerable benefits over macroscale materials.

Combinations of the dimensional, compositional and geometric properties of nanomaterials can reveal unique functionality and enable several applications. With this aim, the synthesis of particular functional nanomaterial with well-defined morphologies that are able to interact with organic molecules is a significant challenging. Functionalization of organic material onto different nanomaterials can generate films that are only one single molecule in thickness. These nanoscale films have been utilized extensively in the engineering of surfaces with well-defined properties.

In the biomedical field, single wall carbon nanotubes (SWCNT) also metallic nanowires have attracted considerable attention due to their properties for the application in optoelectronic and wearable devices. In addition to being less expensive in fabrication cost than other conductive materials, carbon and metallic nanowires also can be bent, stretched, compressed and twisted while remain conductive and reliable. Therefore, films made by nanowires has been reported as the best candidate as a material for future in manufacturing touch screens, solar cells, and other wearable devices. In this paper, we describe the alignment of SWCNTs+DNA on solid surface for the future development and applications of nanowires with its promising properties to achieve flexible optoelectronic and wearable devices.

Introduction

At their fundamental level, many diseases are the result of damage to biological processes that occur at the molecular scale. Nanomedicine is a field that aims to develop treatments at the nanoscale by exploiting the unique properties of nanomaterials and the potential capabilities they offer in biological systems. A defining characteristic of nanomaterials is that they have at least one structural dimension on the order of 100nm or less [1].

Currently nanoparticles have been designed and tested that can act as contrast agents, diagnostic devices or specific drug delivery systems that target both bacterial and viral infections as well as cancerous cells [2]. One of the nanomaterials of great interest to a wide variety of research in the field at the present time is single walled carbon nanotubes (SWNTs).

Single Walled Carbon Nanotubes (SWNTs) have, since their discovery by Iijima [3], been of great interest in many areas of science and engineering due to their unique and remarkable physical and chemical properties. In short, a SWCNT has a combination of high mechanical strength and stiffness, exceptionally good electrical and thermal conductivity [4-6] as well as the intrinsic chemical versatility of many carbon structures allowing many other organic molecules to be linked to the outside of the nanotube [7]. These

properties make SWNTs an ideal material for an enormous range of possible applications: from providing strengthening in composite structures [4,5,8] to the development of new semiconductor devices [9] and their application to nanomedicine [10,11].

There are several significant problems that tends to complicate the use of SWCNTs, and indeed nanoparticles in general, in nanomedicine. First of all, they gave a strong tendency to aggregate both in vitro and in vivo due to strong attractive Van der Waals forces. Therefore, increasing solubility and dispersibility of nanotubes without increasing their toxicity is of great interest. It has been proved that several types of SWNTs functionalization, offers many advantages such as: improving the solubility of the nanotubes, transforming them into more manageable materials, and combining the unique properties of SWNTs with those of other materials [12,13]. Another significant challenging is to obtain a stable surface horizontally alignment of single walled carbon nanotubes (SWCNTs). This is an important step for future development of numerous applications including field-effect transistor, logic circuits, medical sensors, among others. In this paper we provide some insight into the mechanism behind the arrangement/alignment observed in unprecedented dispersed DNA-SWNTs.

Results and Discussion

This paper reports on a new DNA-SWNT hybrid structure formed from loops of double stranded DNA (dsDNA). The details of this wrapping are unpublished and currently subject to a patent (S. Trigueros GB201201207484A). Two remarkable features of the dsDNA-SWNT hybrid structure can be seen, one is the alignment of the nanotubes and second an excellent dispersion of dsDNA-SWNT hybrid nanostructures. Although free nanotubes have been aligned using electric fields [14,15] or both electric and magnetic fields [16], or using printing techniques [17], to the author's knowledge the apparently spontaneous formation of such an alignment is unprecedented in dispersed nanotubes. This unprecedented alignment means that although the purpose of the method's development was to aid in nanotube dispersal for nanomedical applications, the scope of possible uses for its conclusions is far wider.

DNA-SWNT hybrids distribution in different conditions of preparation

Once prepared, samples of DNA-SWNT hybrids were dried and placed in three different physiological solutions. In this work,

we used 100mM $MgCl_2$, Yeast Extract Peptone Dextrose (YPD) and Dulbecco's modified Eagle's medium (DMEM) containing D-glucose (1,000mg) 10% fetal bovine serum (FBS) (Invitrogen), 1% penicillin-streptomycin (Invitrogen) and 0.1% amphotericin B (Sigma-Aldrich). 100mM $MgCl_2$ condition used was the minimum salt concentration necessary to maintain the dsDNA in place around the nanotubes and so is the solution closest to a control available. The latter two solutions were contrasting standard physiological media. YPD is a complete yeast medium needed for yeast cells growth [18] while supplemented DMEM, a complete eukaryotic cell medium commonly used in Fibroblast cell culture [19].

Three raw AFM images shown in Figure 1(A, C & E) of DNA-SWNT hybrids, one in each solution described previously. These were labelled as being of three different conditions A, B and C as shown in Figure 1 for processing and analysis. Each image corresponds solutions are described in caption of Figure 1. Having the conditions unknown at the time of analysis was done to avoid a possible bias that could be created by selecting analysis methods with a view to establishing a significant distinction between the different solutions where perhaps none exists.

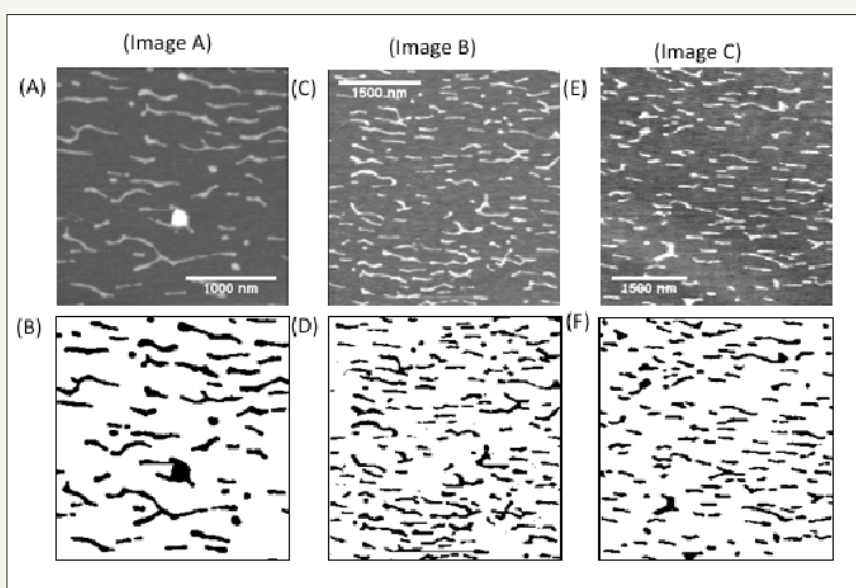


Figure 1: DNA-SWNT images Raw data (A-C-D) The three unprocessed raw AFM images selected for analysis (B-D-F) binarizations produced by the processing described in the text. Image A: DNA-SWNT in 100mM $MgCl_2$. Image B: DNA-SWNT in DMEM. Image C: DNA-SWNT in YPD.

In the development of aligned SWCNTs, size control (length and diameter tubes distribution) physical (spacing between tubes and intertube overlapping) and chemical (metallic or semiconducting) characterization studies are essential.

We show 2D DNA-SWNT characterization according to several analysis related to size and physical (overlapping disposition). Firstly, the intrinsic structural and chemical properties of the individual tubes based on the diameter and length tubes distribution respectively. Differences in diameter and chiral angle lead to difference in electronic structure, resulting in wide-ranging

electronic and optical properties. Secondly density, interdistances and orientation (angles) of the nanotubes on the films influences also the emission. Furthermore, preparation method (determines the geometry of the emitters) and the intrinsic properties of the nanotubes most probably have a significant impact of the field emission performances.

Nanotubes length determination

Theoretical studies have emphasized the importance of nanotube length [20,21]. However, generally only the average

length is used to describe the nanotube length. Furthermore, no formulation is used to describe the distribution of nanotube lengths. This information is not enough for theoretical modelling and final product performance analysis. In particular, in the nanotube reinforced composite, the final mechanical properties, such as tensile strength, elastic modulus, and fracture toughness, are critically dependent on the whole nanotube length distribution rather than the simple mean length. After Image processing analysis (ImageJ software) [22] we identify the DNA-SWNT hybrid in the AFM image tracing the length and export the relevant length information for analysis. The length measurements were acquired through a semi-automatic method. The primary method used the particle analysis function in Image J. This function identifies discrete particles subject to certain constraints in the image and can perform a wide variety of measurements on them individually. First the minimum size of a particle considerable as DNA-SWNT was found and identified as ~1000nm by manually measuring a few smaller particles in the image. Particles smaller than this were excluded from measurement. Additionally, it was clearly necessary

to exclude particles that intersect with the edges of the images as the length of these is unknown.

The available measurement most appropriate to characterize the length of the nanostructures to be measured is Feret's diameter, in ImageJ defined as the longest distance between two points on the particle boundary [22]. This is a good approximation to the length for any straight nanotube; however, for curved nanotubes, or those that intersect other nanotubes, it provides an erroneous measure of length. Such curved or intersecting nanotubes are identified and the automatically acquired data replaced with lengths measured manually using Object, an Image J plugin [22]. ObjectJ creates a transparent measurement layer linked to the image onto which lines can be drawn. By measuring the length of lines drawn on the transparent layer along the axis of any nanotubes in need of manual measurement, the lengths of these nanotubes can be found. The length distributions so collected are compared statistically against each other and against a reference sample of unwrapped nanotubes.

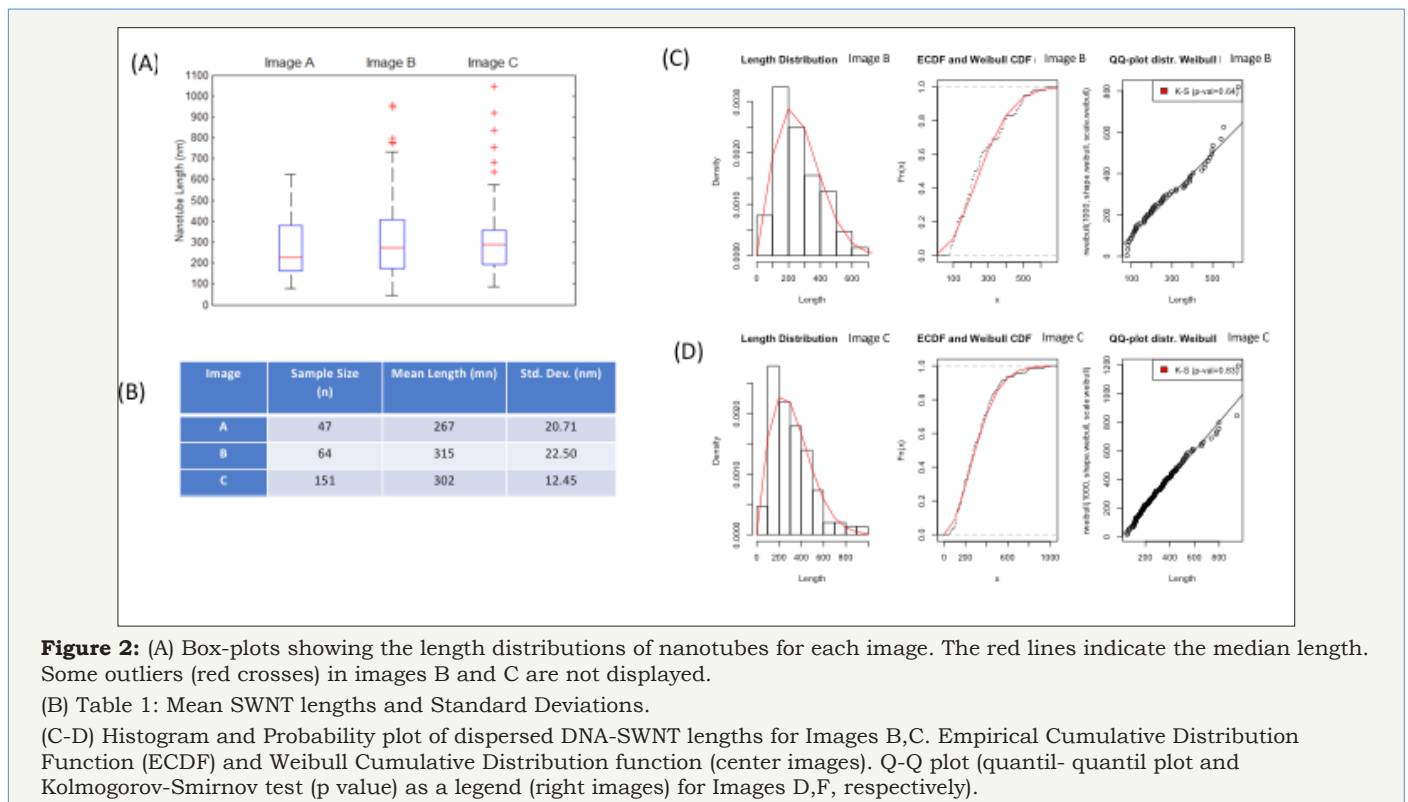


Figure 2: (A) Box-plots showing the length distributions of nanotubes for each image. The red lines indicate the median length. Some outliers (red crosses) in images B and C are not displayed.

(B) Table 1: Mean SWNT lengths and Standard Deviations.

(C-D) Histogram and Probability plot of dispersed DNA-SWNT lengths for Images B,C. Empirical Cumulative Distribution Function (ECDF) and Weibull Cumulative Distribution function (center images). Q-Q plot (quantil- quantil plot and Kolmogorov-Smirnov test (p value) as a legend (right images) for Images D,F, respectively).

Quantified lengths were extracted and plotted into histogram (Figure 2). Considering the shape of the histogram, it appears that the length distribution could be characterized with either a Weibull, Gamma or Log-normal distribution. However, we statistically tested. (Kolmogorov Smirnov goodness of fit test (QQ-plot and K-S pvalue)) the hypothesis that the observed length distribution of SWNTs is a member of a certain parametric family of Weibull distributions.

According to that the probability density function for the Weibull distribution is formulated in

$$f(x) = abx^{(b-1)}exp^{-ax^b}, x > 0 \quad [1]$$

equation [1]; a is the scale parameter and b is the shape parameter. The statistical distribution of the SWNT length helps to reveal the micromechanical characteristics of SWNTs and accurately predict the performance of the final product DNA-SWNT hybrid (out of scope of this paper)

The length effect factor increases with rising tube loading which would keep improving the mechanical properties of the DNA-SWNT hybrid. The gain of the length effect factor from rising tube loading originates from the decreasing of the separator space between SWNTs, which helps to distribute the applied stress in

contrast, the length effect factor reduces quickly when the SWNT rope diameter is increasing.

SWNT-DNA nanotube orientation

At this point we define the orientation of a nanotube as the angle between a line connecting the two ends of the nanotube and the horizontal axis of the image. The method used to measure this parameter was very similar to that used to measure lengths of nanotubes. ImageJ automatically measures the 'Ferret Angle'

when measuring. Feret diameter of a particle; this is defined as the angle anticlockwise from horizontal axis of the image to the Feret diameter of the particle giving an angle between 0° and 180°. For the small minority remaining an additional straight line between the two ends of each nanotube was placed on the ObjectJ transparent layer and the angle between this and the horizontal axis measured using the orientation operation. The distributions of SWNT orientation obtained are then compared to each other as well as to a theoretical distribution (Figure 3).

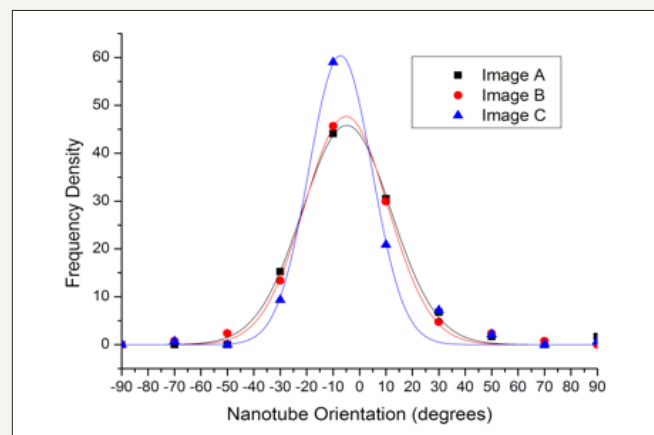


Figure 3: Nanotube orientation direction. Lines show theoretical fits of the form described in the text

The mean orientations are -1.0° , -4.0° and -4.1° for images A, B and C respectively. Considering these values and the measured nanotube orientation density functions presented in Figure 3, it is apparent that a very similar distribution of orientations occurs under all three conditions.

As all nanotubes contain some free electrons and they have been observed to align in the presence of electric fields it seems not unreasonable to consider the DNA-SWNT hybrids on the mica as electric dipoles in two dimensions. The energy of a dipole in a uniform electric field is $-P \cdot E = -PE \cos \theta$ where P is the electric dipole vector and E is the electric field. Applying elementary statistical mechanics [23] the probability of a dipole taking up any particular orientation is therefore:

$$p(\theta) = e^{pE \cos \theta / K_b T} / Z$$

Where K_b is Boltzmann's constant, the absolute temperature and Z the partition function. This model does not take in consideration the interaction that must exist between the nanotubes and even the effect of different nanotube lengths. Thus, fitting function will attempt to capture only the angular dependency of the above probability distribution, taking the form $Ae^{bcos(x-\bar{x})}$. Where θ is the nanotube orientation angle and A , b and \bar{x} are free fitting parameters. This was implemented using the Origin 8.5.1 (Origin (Origin Lab, Northampton, MA) data analysis software. Data obtained (Figure 3) show an apparent good fit achieved with this model around the peaks although it is considerably less accurate away from them, particularly for Image C. Additionally, the tightness of the alignment can be parameterised by the values of the peak width at half maximum: 40° , 39° and 29° respectively. This characterises numerically what is shown at Figure 3, in Image C the

nanotube alignment is tighter than in A or B (note that three AFM samples were obtained in separate days). The apparent preference for a direction a few degrees below the horizontal, as these three images exhibit, is shown on almost all images taken, not just those under study here, removing co-incidence as an explanation.

Nanotube density approach and statistical distribution of horizontal separation distances between nearest neighbors SWNT-DNA

Before any significant analysis of nanotubes separating distances can be made, it is necessary to test if nanotube densities are comparable in the three images. A rough measure of density can be obtained from the Delaunay triangulation where $[r]$ parameter is obtained by measuring the mean length of the edges on the triangulation. $[r]$, representing the mean distance from a nanotube to those surrounding. If there are n particles and A connections between them then on average each particle occupies an area given by:

$$A = \frac{\pi r^2 n}{2k} = \rho^{(-1)}$$

By inverting, a rough density measure is found. In units of particles/nm these are: 1.2×10^{-5} , 9.1×10^{-6} and 8.0×10^{-6} for A, B and C respectively

At this point we analyzed the statistical distribution of horizontal separation distances between nearest neighbors nanotubes by constructing Delaunay triangulation of the centers of the nanotubes. Delaunay triangulation of a set of points is the construction of triangles connecting the points such that no point falls inside the circumcircle of any triangle. This generates triangles connecting with a point to its nearest neighbors. The sides of the

triangles then represent the distances between nearest neighbors. These distances are related to the manner in which the points are distributed in space. Also, the number of nearest neighbors gives information about the coordination. Delaunay triangulation has been used extensively in fields for characterizing distribution in particulate reinforced composites [24].

Here, points are taken at the center of the nanotubes as shown in Figure 4a the center of each linear part of the nanotube. Then a Delaunay triangulation is performed as shown in Figure 4b. The sides of the triangles when collected give the distance between nearest neighbors counted.

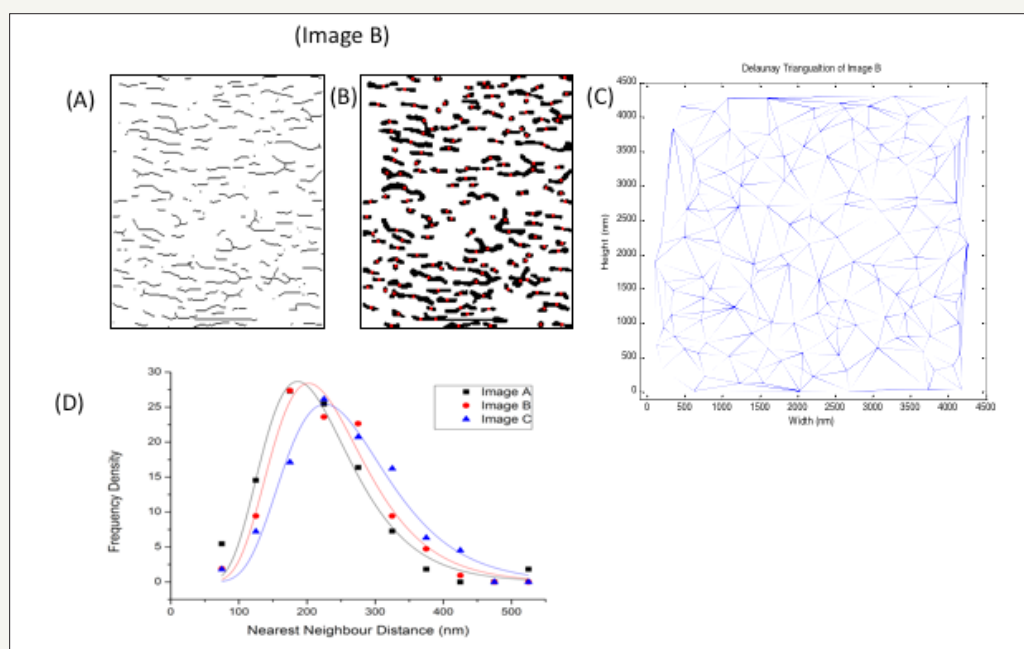


Figure 4: Nanotube density and spacing: Stages to produce a delaunay triangulation.

(A) Skeletonisation of Image B.

(B) Ultimate Eroded points of (A) shown in red superimposed.

(C) Complete Delaunay triangulation of Image B.

(D) Nanotube nearest neighbour distances. Lines show theoretical fits to an appropriate lognormal distribution.

One of the problems of the above method is that it doesn't compensate for the occasional very long edge that is present at the perimeter of the triangulation, as can be seen from Figure 4b. These distort any measure that involves the set of all edges in the triangulation. To avoid this, the set of edges was reduced so that it included only edges that were the shortest edge from one point to any of its neighbours. The distributions thus obtained can then be compared to each other as the length distributions were before looking for statistically significant differences. Therefore, once again the Kruskal-Wallis is performed (p -value=0.0030). According to Dunn post-hoc test, it was found that the only significant difference was between images A and C p -value is 9.36×10^{-4} . Also, it is apparent that a good fit of the distributions is achieved with lognormal model showed in Figure 4d. Referring back to the earlier density data, it is apparent that there is quite a large difference between the nanotube densities in the two images; this may well account for the difference observed.

Experimental Section

Nanotube preparation

Raw, untreated nanotubes were obtained from Sigma-Aldrich

produced via the Chemical Vapour Deposition (CVD) method described above. These nanotubes were then acid treated to reduce their lengths from $\sim 5\mu\text{m}$ to $\sim 500\text{nm}$. A similar method to that of Lui et al. [9], was used. Acid treatment functionalises the nanotubes with carboxylic acid groups (COOH) introducing weak points to the tube where it then can break when energy is added to the solution [14]. To perform the acid treatment, nanotubes were placed in a mixture of highly concentrated sulphuric and nitric acids (3:1, H_2SO_4 : HNO_3) for 90 minutes and before being sonicated. The energy provided by the sonicator overcomes the attractive Van der Waals forces that cause the nanotubes to aggregate as well as providing the energy to break the nanotubes at points where carboxylic acid groups have been added. Finally nanotubes were repeatedly filtered, washed and purified to remove any acid or carbonaceous debris before being placed in solution in ultra-pure Milli-Q water.

Synthesis of DNA-SWNT

Circular molecules of dsDNA were then added to the nanotubes which under certain conditions combine to form the hybrid structure of interest here. Further details of this process are restricted by a patent (S. Trigueros GB201201207484A).

Characterization of synthesized DNA-SWNT

SWNT-DNA hybrids were characterized by atomic force microscopy (AFM) in alternate contact mode. MFD-3D AFM Asylum Research with a silicon tipped cantilever (Olympus OMCL-AC240TS). DNA wrapped nanotubes were prepared in the three solutions and placed on flat pieces of freshly cleaved Mica allowing to dry in a laminar air flow. Once as much water as possible had been allowed to evaporate from samples they were imaged with an Atomic Force.

Conclusion

This work set out with two main purposes: First, to characterize the novel and unexpected properties of the dsDNA-SWNT hybrid nanostructures using image analysis techniques. Second, to answer the question of whether we can use these methods to provide some insight into the mechanism behind the arrangement observed.

The first variable studied was the length of the nanostructures observed. Majority of nanotubes studied had a length range of 100-500nm with a mean length around 305nm. This compares agreeably with the known mean length of the nanotubes before treatment with DNA of 315(12)nm [unpublished data] indicating that the process of sample preparation does not have a significant bias towards different lengths of nanotube. When the length distributions obtained were compared against each other, no significant differences in distribution were identified. This indicates that the DNA-SWCNTs complex is equally stable in all environments tested and is therefore not disrupted by medium composition.

A remarkable feature of the nanostructure under study is the apparently spontaneous alignment of the dispersed nanotubes. This feature was investigated by measuring the nanotubes orientation. In this work we show that although there is no known cause of the alignment, as in all three images (representing different sample conditions) it is within a few degrees of the same axis, it is likely that it is being caused by an unknown external effect. If the nanotubes were adopting an internal minimum energy state only defined by their mutual interactions, one would expect less consistency in alignment direction and possibly a 'domain' structure as seen in ferromagnetic materials. Also, we shown the alignment in YPD is tighter than in $MgCl_2$ or DMEM. However, a better knowledge on alignment mechanism will be needed for further interpretation.

The third characterization variable was the nearest neighbor edges of the Delaunay Triangulation of the images. Here a lognormal fit was found to be appropriate; this is in line with the observations of previous studies into the dispersion of nanoparticles. Although the methods of these investigations are different. When sample distributions from the three conditions under study here were compared, a statistically significant difference was found between $MgCl_2$ condition and YPD. Although this may be an effect of variations on nanotube density between both conditions.

Acknowledgment

Authors are grateful to Daniel Johnson for his support on Imaging analysis and Sonia Antoraz Contera for her support on

AFM. S.C was supported by 2014SGR464 awards from Generalitat de Catalunya's Agency (AGAUR) and BFU2015-64699-P MINECO. S.T was supported by EPSRC IAA D4D00620. Authors also acknowledge support from the Oxford Martin School.

References

- Chopra N, Gavalas VG, Hinds BJ (2007) Functional one-dimensional nanomaterials: applications in nanoscale biosensors. *Anal Lett* 40(11): 2067-2096.
- Kim B, Rutka J, Chan WC (2010) Nanomedicine. *New England Journal of Medicine* 363(25): 2434-2434.
- Iijima S (1991) Helical microtubes of graphitic carbon. *Nature* 354: 56-78.
- Thostenson E, Ren Z, Choi T (2001) Advances in the science and technology. *Composites Science and Technology* 61(13): 1899-1912.
- Ruoff R, Lorents D (1995) Mechanical and thermal properties. *Carbon* 33(7): 925-930.
- Fischer J, Johnson A. Current opinion in solid state and materials science. 4: 28
- Lu X, Chen Z (2005) Curved Pi-conjugation, aromaticity, and the related chemistry. *Chemical Reviews* 105(10): 3643-3696.
- Coleman J, Kahn U, Gun'ko Y (2006) Mechanical reinforcement of polymers. *Advanced Materials* 18(6): 689-706.
- Lui S, Brisano A (2007) Selective crystallisation of organic semiconductors, advanced functional materials. 17(15): 2891-2896.
- Fabbro C, Ali-Boucetta H (2012) Targeting carbon nanotubes against cancer. *Chemical Communications* 48(33): 3911-3926.
- Ji S, Lui C (2010) Carbon nanotubes in cancer diagnosis. *Biochimica et Biophysica Acta* 1806(1): 29-35.
- Yamamoto Y, Fujigaya T (2010) Fundamental properties of oligo double-stranded DNA/single-walled carbon nanotube nanobiohybrids. *Nanoscale* 2(9): 1767-1772.
- Daniel S, Rao TP, Rao KS (2007) A review of DNA functionalized/grafted carbon nanotubes, and their characterization. *Sensors and Actuators B: Chemical* 122(2): 672-682.
- C Ma W, Zhang Y (2008) Alignment and dispersion of functionalized carbon nanotubes in polymer composites induced by an electric field. *Carbon* 46(4): 706-710.
- Monti M, Natali M (2012) The alignment of single walled carbon nanotubes in an epoxy resin by applying a DC electric field. *Carbon* 50(7): 2453-2464.
- Arjmand M, Mahmoodi M (2011) Electrical and electromagnetic interference shielding properties of flow-induced oriented carbon nanotubes in polycarbonate. *Carbon* 49(11): 3430-3440.
- Zhang Q, Wei N (2017) Recent developments in single-walled carbon nanotube thin films fabricated by dry floating catalyst chemical vapor deposition. *Top Curr Chem (Cham)* 375(6): 90.
- Difco (2000) Yeast extract-peptone-dextrose (YPD) agar yeast extract-peptone-dextrose (YPD) broth. Difco™ & BBL™ Manual p. 10.
- Raman A, Trigueros S, Cartagena (2011) Mapping nanomechanical properties of live cells using multi-harmonic atomic force microscopy. *Nature Nanotechnology* 6(12): 809-814.
- Cao G, Chen X (2006) Mechanisms of nanoindentation on single-walled carbon nanotubes: The effect of nanotube length. *Journal of Materials Research* 21(4): 1048-1070
- Wang S, Liang Z (2006) Statistical characterization of single-wall carbon nanotube length distribution. *sNanotechnology* 17(3): 634-639.

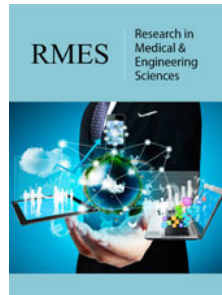
22. Rasband WS (1997-2018) ImageJ, US National Institutes of Health, Bethesda, Maryland, USA,
23. Blundell S, Blundell K (2010) Concepts in thermal physics (2nd edn), OUP, UK, 2010: 217.
24. SR Bakshi, RG (2009) Batista quantification of carbon nanotube distribution and property correlation in nanocomposites. Composites 40: 1311-1318.



Creative Commons Attribution 4.0
International License

For possible submissions Click Here

[Submit Article](#)



Research in Medical & Engineering Sciences

Benefits of Publishing with us

- High-level peer review and editorial services
- Freely accessible online immediately upon publication
- Authors retain the copyright to their work
- Licensing it under a Creative Commons license
- Visibility through different online platforms